

## Morphofunctional Changes in Frozen-Thawed Sperm of *Apis Mellifera* Linnaeus Drones

A. N. Gulov<sup>a,\*</sup> and Y. E. Bragina<sup>b,\*\*</sup>

<sup>a</sup> Federal State Budgetary Scientific Institution “Federal Beekeeping Research Centre,” Rybnoe, Ryazan region, 391110 Russia

<sup>b</sup> A.N. Belozersky Research Institute of Physico-Chemical Biology, Lomonosov Moscow State University, Moscow, 119992 Russia

\* e-mail: blee3@yandex.ru

\*\* e-mail: bragor@mail.ru

Received May 31, 2022; revised July 6, 2022; accepted August 29, 2022

**Abstract**—Instrumental insemination of queen bees using cryopreserved sperm is an important biotechnological tool to address the issues of contemporary beekeeping. Long-term cryopreservation is detrimental to sperm function and drone fertility, killing more than 50% of the sperm during the process. Prediction of cryopreservation damage from freezing drone semen remains elusive. The purpose of this study was to assess the impact of long-term cryopreservation in “Kakpakov diluents” (C46) on morphometric measurements of sperm head of the *Apis mellifera* L. and ultrastructure. For the experiment, sperm samples from the cryobank of the Federal Beekeeping Research Centre (Russia), frozen since 1993, 2011 and 2013 were used. In the present study, it was found out that cryopreservation had a considerable impact on the drone sperm head morphometry. Sperm head measurements of cryopreserved samples were significantly lower compared with the extended sample for morphometric measurements of the nucleus area  $3.55 \pm 0.12$ ,  $4.07 \pm 0.1$ ,  $4.31 \pm 0.04$  ( $5.57 \pm 0.03$ , respectively); nucleus perimeter  $10.57 \pm 0.11$ ,  $11.11 \pm 0.13$ ,  $11.59 \pm 0.05$  ( $11.72 \pm 0.06$ , respectively); nucleus length  $4.66 \pm 0.05$ ,  $4.82 \pm 0.06$ ,  $5.07 \pm 0.02$  ( $5.22 \pm 0.03$ , respectively); nucleus acrosome length  $3.72 \pm 0.08$ ,  $3.65 \pm 0.08$ ,  $3.96 \pm 0.05$  ( $4.24 \pm 0.04$ , respectively). Cryopreserved and thawed spermatozoa revealed changes in ultrastructure such as vacuolation of the axoneme, intranuclear vacuoles, and loss of the derivative’s mitochondria. These details provide valuable data for further experiments on modification of the composition of cryomedium to minimize cryodamage in the semen of honey bee drones.

**Keywords:** cryopreservation, drone, morphometric parameters, spermatozoon, ultrastructure

**DOI:** 10.3103/S1068367422060040

### List of abbreviations

Mit 1	larger mitochondrial derivative,
Mit 2	smaller mitochondrial derivative,
Mp	microtubule pattern,
Ax	axoneme,
Ab	accessory bodies,
C	centriolar region,
p	paracrystalline region,
N	nucleus.

such as instrumental insemination of queen bees and conservation of drone sperm.

Most reproductive qualities of an instrumentally inseminated queen bee depend on the fertility of drones. Cryopreservation makes it possible to create sperm banks of high-value breeding drones of honey bees and preserve genetic material for selection for a long time. The main purpose of cryopreservation of drone sperm is to use such sperm for instrumental insemination of queen bees, which will reproduce many worker bees, as well as queens, do after natural mating. In this case, instrumental queens can be obtained at the beginning of the beekeeping season. Drone sperm has been successfully preserved by cryopreservation in recent years [1–3].

The analysis of cryopreserved and thawed sperm from honey bee drones is based on an assessment of standard semen parameters: sperm motility, viability, and concentration. Wegener et al. (2012) [4] concluded that a new test based on the wastage of the glycolytic enzyme (glucose-phosphate-isomerase (GPI))

**INTRODUCTION**

Today the state of the gene pool of honeybees is one of the main causes of the beekeeping crisis in the world. Conservation of genetic resources of honey bees is a pressing problem of the growing ecological crisis. There is an urgent need to use biotechnological methods for preserving the gene pool of honey bees,

from damaged cells correlates with the number of spermatozoa that reached the queen bee spermatheca ( $r = -0.61$ ). Alcay et al. [5] concluded that HOS tests and water are suitable and simple measures of the functional integrity of the sperm plasma membrane.

Little attention is paid to the study of morphometric parameters of individual structural elements and ultrastructural damage in spermatozoa.

A variety of cryopreservation factors can cause structural changes in sperm [6]. These changes significantly reduce sperm motility, plasma membrane functionality, acrosome integrity, and sperm fertility [7–9]. Damage to the acrosome and changes in chromatin condensation evoked by freezing and thawing of the gamete [10] influence the morphology of spermatozoa and the morphometric parameters of individual structural elements. Previous studies have shown the effect of deep freezing on the morphometry of sperm head of an ox [10], a human [11], a stallion [12], a dog [13], and a red deer [14]. In these studies, frozen and thawed sperm heads were significantly smaller than freshly harvested heads. However, experiments with goats have revealed that cryopreservation did not cause significant differences in sperm head size [15]. Probably, these contradicting results may be contingent on the sensitivity of the species' sperm to the freezing process or different cryopreservation protocols.

Sperm morphology correlates more closely with fertilization rate, rather than with sperm concentration and motility [16, 17].

Light and fluorescence microscopy of frozen and thawed sperm cannot reveal significant ultrastructural damage in the sperm. Electron microscopy is a perfect method for ultrastructural analysis of the functional state of spermatozoa and the diagnosis of damage in gametes after cryopreservation. Atroshchenko et al. (2017) [18] concluded that cryopreservation of sperm leads to dispersal of acrosomal contents and enzymatic deficiency of the acrosome. The authors observed mitochondrial pathologies in <10% of spermatozoa. The sperm axoneme was resistant to cryopreservation. Peripheral dense fibrils and fibrous membrane of the axoneme were not damaged by freezing and thawing [18]. Kandiel et al. [19] concluded that the freezing and thawing process caused significant ultrastructural changes in the acrosomes and middle pieces, including rupture of plasma membrane and acrosomal membrane with or without dispersal of acrosomal contents and a decrease in the electron density of mitochondria.

Ultrastructure is not a very useful approach for daily sperm assessment for a number of reasons, such as technically challenging limited observation and costs. Quantitative TEM analysis is difficult to perform due to the cost of the procedure and the fragility of tissue under prolonged exposure to the electron beam [20]. In the present study, quantitative TEM analysis

was used to assess the cryobanking of honeybee drone sperm in “Federal beekeeping research centre” (Russia).

The given research work is aimed at assessing the effect of cryopreservation on the morphometric parameters of individual structural elements of *A. mellifera* L. drone spermatozoa and ultrastructure.

## MATERIAL AND METHODS

### *Location and Characteristics of the Study Area*

The collection of fresh semen was carried out at the Federal Beekeeping Research Centre (Ryazan Region, Russia). Sperm samples were examined in the laboratory of selection and molecular genetics research of honeybees of the FBRC in 2018.

### *Semen Collection and Processing*

Sperm were collected on 25–30 days post-emergence drone of subspecies *A. mellifera* L. Ejaculation was manually induced by pressure on the chest [21], and semen were collected in glass capillaries using a Harbo Schley insemination syringe (ref. 104) and Schley-System model 1.04 (A & G Wachholtz, Germany). The average semen volume collected per drone was close to 1  $\mu$ L. Semen was obtained while filling a 100  $\mu$ L glass capillary for subsequent cryopreservation.

### *Diluents*

To conduct the experiment, we used sperm samples frozen for insect cells medium by V. Kakpakov (C46) with 10% dimethyl sulfoxide (DMSO) [3] from the FBRC cryobank (Ryazan region, Russia). For the experiment, 5 frozen semen samples preserved since 2013 (each sample had 30  $\mu$ L of diluted semen in straws), and 2 samples since 2011 (each sample had 100  $\mu$ L of diluted semen in a Nunc Cryotube) and 2 samples since 1993 (each sample had 100  $\mu$ L of diluted semen in a Nunc freezer tube) were obtained. The samples were thawed by immersion in a water bath at 34°C for 1 min. After freezing and thawing, 1 mL of C46 was added to the samples. The samples were left in this form for 10 min. After 10 min, the samples were shaken and centrifuged on a Mini Spin Eppendorff (Germany) for 3 min/3000 rpm. After centrifugation, the supernatant fluid was removed from the test tube and 1 mL of C46 was added. The samples were left in this form for 5 min. After 5 min, the samples were shaken and centrifuged for 3 min/3000 rpm. After centrifugation, the supernatant fluid was removed from the test tube and the quality of the thawed semen was assessed.

### *Evaluation of Seminal Quality in a Fresh and Thawed State*

The variables assessed in fresh semen and the thawed one were morphometric parameters of individual structural elements of sperm. After thawing, the sperm viability and ultrastructure were additionally studied.

Motility was assessed as “great” if it was indistinguishable from fresh semen. A “good” score was given if the motility was noticeably less than that of fresh sperm, while a “bad” score was given if the sperm were just slightly moving [1].

### *Morphometric Assessment of Sperm Heads*

Diff Quik staining (ABRIS+, St. Petersburg, Russia) was used to study the morphometric parameters of sperm heads. Diff Quik stain is used to stain smears of animal's semen [13, 22–24]. Microscopic slides were prepared from each extended sample (upon dilution) by placing 20  $\mu\text{L}$  of the sperm samples on the clear end of a frosted microscope slide and dragging the drop across the slide. Semen smears were air-dried. Fixation of the smear in solution no. 1 was performed for—10 min, staining in solution no. 2 (eosin)—for 15 min, and then the dried smear was stained in solution no. 3 (thiazine)—for 10 min [22]. After staining, the slides were washed in buffer (pH 6.8) for 2 min. Sperm slides were examined with an Altami-LUM 1 LED microscope using oil immersion at a magnification of 2000 $\times$ . Sperm images were taken on each of the slides with Canon 1300D digital cameras (Canon Inc., Tokyo, Japan). Sperm images and morphometric parameters were studied using Altami Studio software version 3.5 (Altami LLC, St. Petersburg, Russia). The measurements for nucleus area, nucleus perimeter, nucleus length, and acrosome length were acquired from 200 images. Acquiring 200 images assures that a minimum of 150 properly measured sperm heads is analysed. Improperly measured sperm heads were deleted from the analysis. The sperm cells were randomly selected for the morphometric analysis. The measurements of each sperm head and sperm treatment were saved in an Excel (Microsoft Corporation, USA)—compatible database for further analysis.

### *Sperm Viability*

Live/dead sperm staining was assessed using the Locke & Peng (1990) [25] double fluorescent staining protocol, with our modification. Fluorescent spots Hoechst 33258 (H3258) (catalog no. O150; Pan-Eco, Russia) and PI (catalog no. 25535-16-4; Sigma-Aldrich, USA) were used. Working solutions of fluorochromes were prepared in Tris buffer pH 8.8 [26]. The final concentration of H3258 is 5  $\mu\text{g}/\text{ml}$  and PI is 10  $\mu\text{g}/\text{mL}$  [25]. The sperm suspension was additionally diluted in Tris buffer pH 8.8 to achieve a final ratio of 1:100. The stained gametes were counted at a mag-

nification of  $\times 400$  using an Altami-LUM 1 LED microscope (Altami LLC, Russia). A total of 200 spermatozoa were counted. The microscope was equipped with a Hg lamp and corresponding filter cubes for UV excitation H3258: 340–380 nm (UV block) and a luminescence range of 430 nm. PI of green excitation: 530–560 nm (block G) and the luminescence range is 580 nm. Living cells were stained in blue and dead cells were red.

### *Electron Microscopic Observations*

For electron microscopy, fresh and frozen and thawed sperm samples were diluted with isotonic NaCl solution in a ratio of 1:10 and a fixative solution was 200  $\mu\text{L}$  added 2.5% glutaraldehyde solution (Ted Pella Inc., USA), which had been prepared in 0.1M cacodylate buffer (pH 7.2) (“Sigma,” USA) for electron microscopy. The sample tube was centrifuged for 15 min/1000 rpm. After centrifugation, the supernatant fluid was removed and the pellet was fixed with fixative solution. Further, it was fixed with a 1% solution of osmic acid (Serva, Germany) and poured into an epon (Fluka, Germany). Ultrathin sections were obtained on an UltraCut III microtome (Reichert Jung Optische Werke AG, Austria) and stained with an aqueous solution of uranyl acetate and lead citrate (Serva, Germany). The stained sections were examined under transmission electron microscope JEM1400 (Jeol, Japan). The visual appearance of spermatozoa was studied at  $\times 5000$  magnification, acrosome, chromatin nuclei, and mitochondria derivative were examined at  $\times 16000$ – $18000$ , axoneme abnormalities on cross-sections of flagella were observed at  $\times 20000$ – $25000$  magnification. In each sample, at least 100 sex gametes were analyzed.

### STATISTICAL ANALYSIS

In the present study, the author has not performed a quantitative analysis of TEM due to the cost of the procedure.

Statistical analysis was used to assess the morphometric parameters of individual structural elements of spermatozoa. The data were examined by factorial ANOVA. The normality of distribution was checked using Shapiro–Wilk statistics. Group differences were compared using Tukey test. Effects were considered significant at  $p \leq 0.05$ . All analyses were performed using STATISTICA version 13.0 split plot design (StatSof, Moscow, Russia).

### RESULTS

Spermatozoa previously frozen with C46 diluents were slightly motile during the thawing (poor motility) than fresh semen. The gamete in liquid nitrogen storage preserved since 1993 has ensured long-term storage of sperm membranes (sperm viability) (Fig. 1).

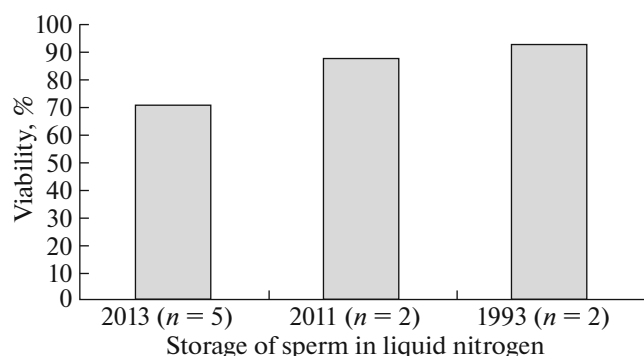


**Fig. 1.** Percentage of drone freezing and thawing sperm viability integrity during cryopreservation procedure.

When evaluating the morphometric parameters of individual structural elements of spermatozoa, a lot of abnormalities in the structure of the head were found (Fig. 2).

A lot of sperm head anomalies have been observed in liquid nitrogen storage of gametes since 2013, which were frozen in straws.

Morphometric parameters such as nucleus area and perimeter, nucleus length were significantly ( $p < 0.05$ ) less in cryopreserved semen than in fresh expanded semen (Table 1).

Significant effects of cryopreservation treatment ( $p < 0.05$ ) were found between the liquid nitrogen storage groups of 1993 and 2013 gametes in terms of the size of nucleus area and perimeter, and nucleus length. We observed ultrastructural cryodeficits, including damage to the axoneme and mitochondria, and the nucleus. The flagellum of the honeybee sperm

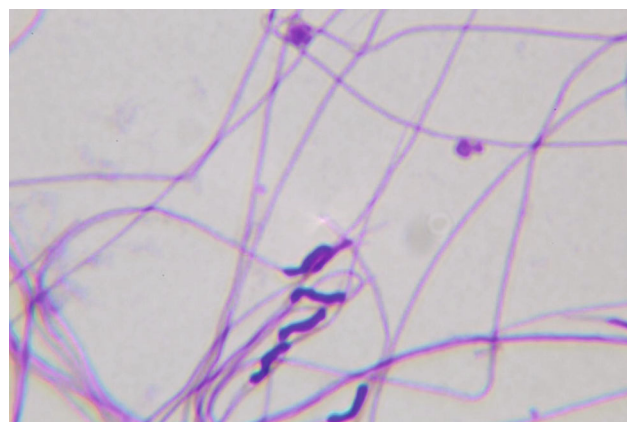


**Fig. 2.** Morphological defects in sperm nucleus formation (experimental Diff Quick staining).

consists of two derivatives of mitochondria, an axoneme and two additional triangular bodies (Figs. 3, 4).

The axoneme follows a typical 9+9+2 microtubule pattern; including 9 external singles accessory tubules, 9 doublets, and 2 single central microtubules (Fig. 4).

We have observed a larger mitochondrial derivative in frozen and thawed sperm that is not related to the axoneme (Fig. 5).

Observing Fig. 6, it can be concluded that the axoneme does not have a small and large mitochondrial derivative (flagellum fragmentation).

A damaged centriolar region (C) with an electron lucent interior may indicate loss of content (Fig. 7).

The p-region in a larger mitochondrial derivative is formed by paracrystalline material [27–29]. Electron

**Table 1.** Mean sperm head measurements for extended and cryopreserved drone semen

Morphometr parameters	Sample			
	extended (fresh semen)	liquid nitrogen storage with (year)		
		1993	2011	2013
Acrosome lenght, $\mu\text{m}$	$4.24 \pm 0.04^a$ (3.61–5.26)	$3.96 \pm 0.05^b$ (3.06–5.97)	$3.65 \pm 0.08^c$ (3.22–4.82)	$3.72 \pm 0.08^d$ (3.25–4.25)
Sperm nucleus lenght, $\mu\text{m}$	$5.22 \pm 0.03^a$ (4.66–6.57)	$5.07 \pm 0.02^b$ (4.00–6.37)	$4.82 \pm 0.06^c$ (4.4–5.51)	$4.66 \pm 0.05^{db}$ (3.86–5.79)
Nucleus perimeter, $\mu\text{m}$	$11.72 \pm 0.06^a$ (10.8–14.2)	$11.59 \pm 0.05^a$ (9.63–14.5)	$11.11 \pm 0.13^b$ (9.92–12.3)	$10.57 \pm 0.11^{cab}$ (8.89–12.8)
Nucleus area, $\mu\text{m}^2$	$5.57 \pm 0.03^a$ (4.39–6.58)	$4.31 \pm 0.04^b$ (2.5–6.21)	$4.07 \pm 0.04^c$ (3.11–4.86)	$3.55 \pm 0.12^{dcb}$ (2.23–5.64)

Data are expressed as means  $\pm$  SD. a, b, c, d:  $P < 0.05$ .



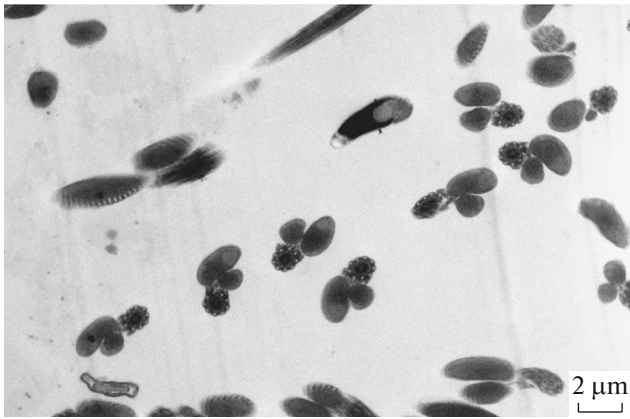


**Fig. 3.** Various flagella cross sectioned anteriorly. Scale bar—2 μm.

microscopic examination revealed damage of the structure of the paracrystalline region (Fig. 8).

The nucleus of frozen and thawed spermatozoa also had lesions with an electron lucent interior part, it looks as if it is vacuolated (Fig. 9) and with invagination in the nucleus (Fig. 10).

Observing Fig. 11, we can conclude that the axoneme has a damaged area of the body (non-compact axoneme content).

## DISCUSSION

The drone of *A. mellifera* has filamentous spermatozoa with a length of 250–270 μm and a head length of 8–10 μm, and a total acrosomal length of 5 μm [30]. Several recent studies describe seasonal variation and the association of morphology and standard parameters of drone sperm. In the study by Gontarz et al. [31]

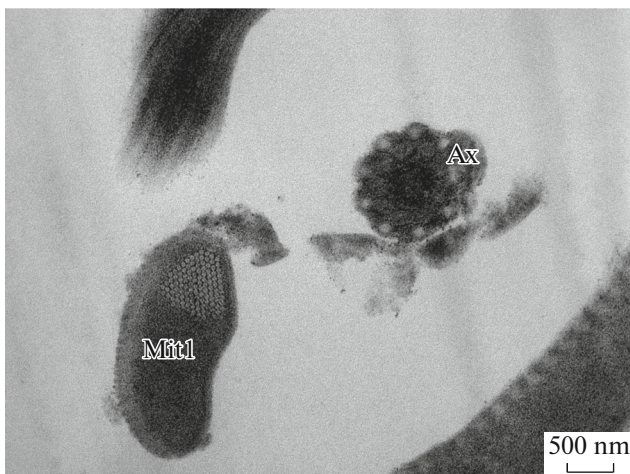


**Fig. 5.** Larger mitochondrial derivative separated from axoneme. Mit 1—larger mitochondrial derivative, Ax—axoneme. Scale bar—500 μm.

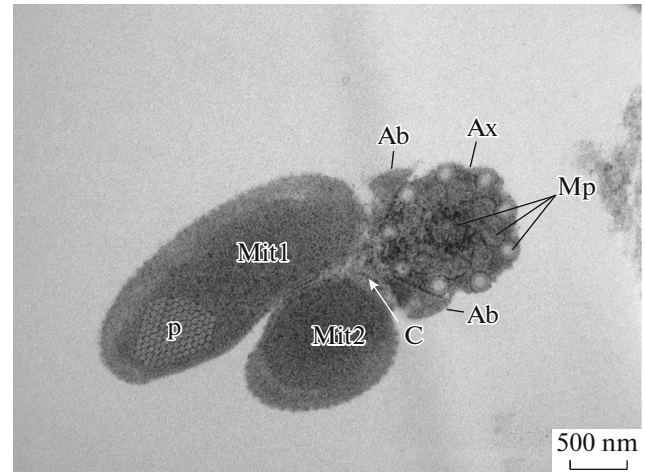


**Fig. 4.** A flagellum cross sectioned at the level of two mitochondrial derivatives. Mit 1—larger mitochondrial derivative, Mit 2—smaller mitochondrial derivative, Mp—microtubule pattern, Ax—axoneme, Ab—accessory bodies, C—centriolar region, p—paracrystalline region. Scale bar—500 μm.

the sperm of *A. m. carnica* were evaluated. In the study by Power et al. [32] the spermatozoa of *A. m. ligustica* were evaluated. The authors [31, 32] investigated the morphometric parameters of spermatozoa such as total sperm length, tail length, head length, nucleus length, acrosome length. Spermatozoa *A. m. ligustica* turned out to be smaller; their average total length was  $230.8 \pm 17.22 \mu\text{m}$  [32]. The average total length of spermatozoa *A. m. carnica* was  $273.5 \pm 16.58 \mu\text{m}$  [31]. In the current study, we evaluated the morphometric parameters of the sperm head only.

In the study by Gil et al. [33] a significant connection of sperm swimming speed with several morphometric parameters of the head and midsection were

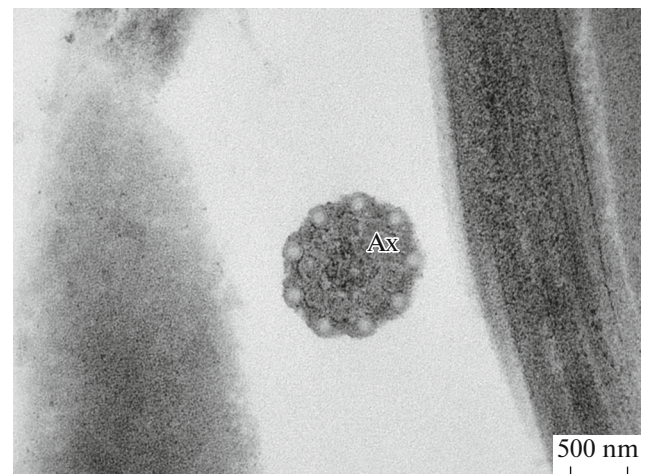


**Fig. 6.** The axoneme lacks a smaller and larger mitochondrial derivative. Ax—axoneme. Scale bar—500 μm.



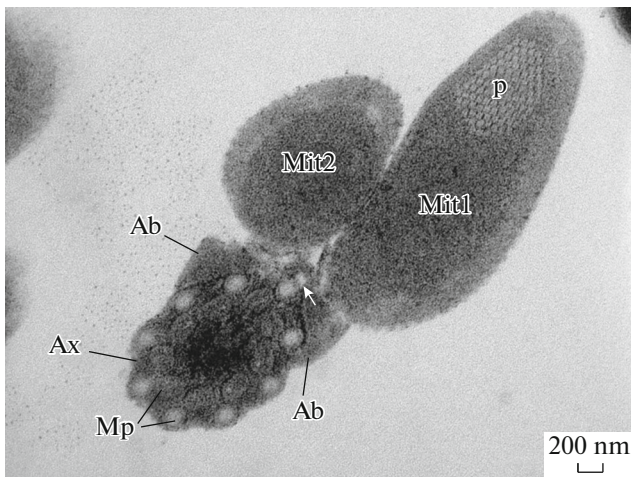


**Fig. 7.** Damaged centriolar region with electron lucent interior (white arrow). Mit 1—larger mitochondrial derivative, Mit 2—smaller mitochondrial derivative, Mp—microtubule pattern, Ax—axoneme, Ab—cessory bodies, p—paracrystalline region. Scale bar—200 nm.

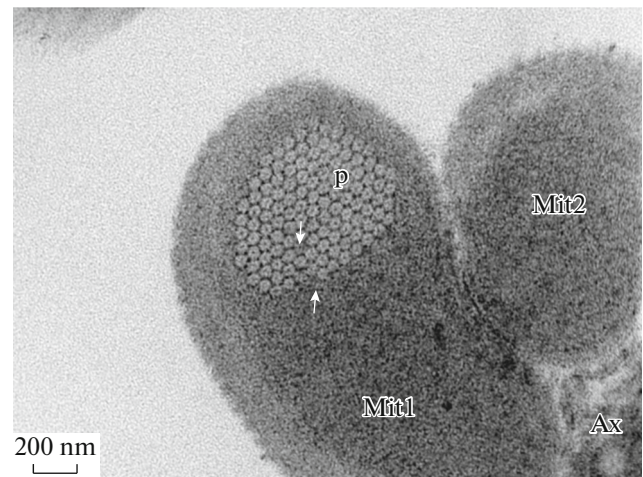


**Fig. 8.** Damage to the structure of the paracrystalline region (white arrow) of a larger mitochondrial derivative. Mit 1—larger mitochondrial derivative, Mit 2—smaller mitochondrial derivative, Ax—axoneme, p—paracrystalline region. Scale bar—200 nm.

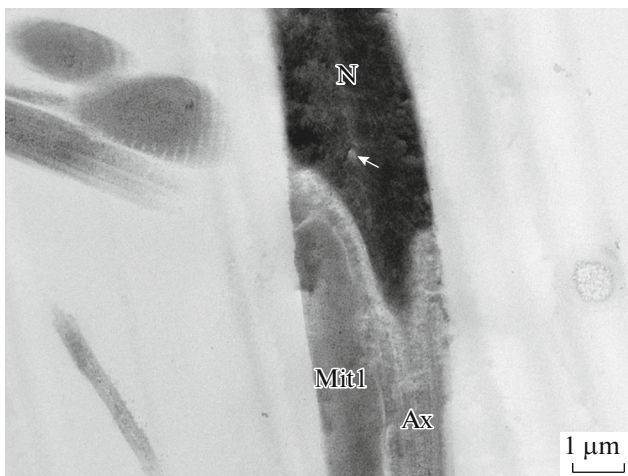


**Fig. 9.** Electron lucent interior inside the sperm nucleus that appears vacuolated (white arrow). Mit 1—larger mitochondrial derivative, Ax—axoneme, N—nucleus. Scale bar—1 μm.



**Fig. 10.** Spermatozoon showing invagination in the nucleus (white arrow). N—nucleus. Scale bar—1 μm.

found. Motility is generally considered to be one of the most important sperm characteristics associated with drone fertility. Motility is an expression of the viability and structural integrity of the sperm [33].

Head morphometric parameters and ultrastructure of frozen and thawed spermatozoa of drones have not been described. This is the first report evaluating the effect of long-term cryopreservation on the morphometric parameters of individual structural elements of spermatozoa and ultrastructure. In the present study, the cryopreservation of drone spermatozoa had a significant effect on the morphometry of the sperm heads. Sperm measurements in cryopreserved samples

were significantly lower than in expanded sample for morphometric measurements of nucleus area, nucleus perimeter, nucleus length. The changes caused by cryopreservation identified in the given study were similar to changes in the morphometric parameters of the sperm head of different mammalian species [10–14]. Cryopreservation methods are known to have a great impact on post-traumatic motility, viability [4, 34], and acrosomal status [35] of spermatozoa. The fertility of the semen sample is also influenced by cryopreservation methods [1, 36]. Changes in the size of the sperm head as a result of cryopreservation can be caused by acrosomal damage [12] or altered chro-



**Fig. 11.** Damage (fracture) to a larger mitochondrial derivative (black arrow). Mit 1—larger mitochondrial derivative, Ax—axoneme, N—nucleus. Scale bar—1  $\mu\text{m}$ .

matin condensation [37]. In the study by Royere et al. [37], it was found that the surface area of the sperm heads tends to decrease after freezing and thawing. This decrease in surface area was connected with changes in the structure of sperm chromatin. Royere et al. [37] hypothesized that cryopreservation induces overcondensation of sperm chromatin.

Progressive dehydration of the sperm during cooling and freezing may be a possible explanation for the decrease in morphometric parameters of the head after cryopreservation [38]. A number of stages in a cryopreservation protocol can affect the extent of sperm damage, including cryoprotectant levels, cooling and freezing rates, and thawing methods [10].

In the current research, evaluation of spermatozoa with a transmission electron microscope has allowed revealing damaged cellular structures after cryopreservation in >50% of the examined spermatozoa. In the present study, the presence of intranuclear vacuoles was uncovered. The structure of the axoneme and mitochondria of the derivative was also influenced by the freezing and thawing processes. Transmission electron microscope images revealed vacuolation of the axoneme and loss of mitochondria derivative of the frozen and thawed sperm. Damage to the mitochondria of a derivative during freezing and thawing can lead to a decrease in the mitochondrial membrane potential [39]. The changes caused by cryopreservation and found in the present study were similar to changes in some ultrastructures of fish spermatozoa [40] and different mammalian species such as llamas [39], horses [18], and rams [41]. In the study by Atroshchenko et al. [18] the authors found many spermatozoa with acrosome fragmentation due to false acrosome reaction, with acrosome hyperplasia (non-compact acrosome content), and nuclear changes and vacuolization of chromatin. In the study by Balamuru-

gan et al. [40], it is shown that freezing and thawing caused various ultrastructural changes, such as damage to the plasma membrane around the sperm head, flagellum fragmentation, and complete flagellum loss in fish sperm. In the study by Zampini et al. [39], acrosome damage, loss of mitochondria, disorganization of the axoneme and periaxonemal structures, and invagination in the nucleus of llama spermatozoa were observed with the help of TEM. In the study by Keskin et al. [41] mainly cryodamage to the membrane, as well as mitochondria (electron-lumen matrix) and axoneme (loss of axoneme doublets) cryo-damage were observed in ram sperm STEM. Vesiculation in acrosomal membranes and loss of acrosomal content observed in the study [18, 37, 39–41] with frozen-thawed semen could be the result of an acrosomal reaction. In the current research, we have not detected the drone sperm acrosome using a transmission electron microscope and have not evaluated the effects of cryopreservation. The observed ultrastructural changes indicate that our freezing protocols for drone semen need to be reconsidered, evaluating various diluents and cryoprotectants from the ultrastructural perspective. In conclusion, it can be said that the ultrastructure of the first frozen and thawed spermatozoa of honeybee drones and the ultrastructure of damage caused by long-term cryopreservation are characterized by the freezing procedure. The transmission electron microscope has allowed us to detect several ultrastructural sperm lesions that would not have been noticed by routine baseline assessments. Electron microscopic observation of frozen and thawed spermatozoa can help optimize the cryomedium, composition, and other important factors to minimize cryo-damage [40]. Further research should focus on reducing damage to the ultrastructure of sperm during freezing to improve cryopreservation protocols for drone sperm.

#### CONFLICT OF INTEREST

The authors declare that they have no conflicts of interest.

#### REFERENCES

1. Hopkins, B., Herr, C., and Sheppard, W., Sequential generations of honey bee (*Apis mellifera*) queens produced using cryopreserved semen, *Reprod., Fertil. Dev.*, 2012, vol. 24, pp. 1079–1083. <https://doi.org/10.1071/rd11088>
2. Hopkins, B., Rajamohan, A., Danka, R., and Rinehart, J., A non-activating diluent to prolong in vitro viability of *Apis mellifera* spermatozoa: Effects on cryopreservation and on egg fertilization, *Cryobiology*, 2019, vol. 92, pp. 124–129. <https://doi.org/10.1016/j.cryobiol.2019.11.045>
3. Kakpakov, V., Kabashova, O., Khmelev, A., Kakpakova, E., and Borodachev, A., The long-term cryobiological preservation of the drone sperm and of the honey bees embryos, in *The Materials of the 34 International*



- Apimondia Beekeeping Congress*, Lousanne, 1995, pp. 102–103.
4. Wegener, J., May, T., Knollmann, U., Kamp, G., Müller, K., and Bienefeld, K., *In vivo* validation of *in vitro* quality tests for cryopreserved honey bee semen, *Cryobiology*, 2012, vol. 65, no. 2, pp. 126–131. <https://doi.org/10.1016/j.cryobiol.2012.04.010>
  5. Alcay, S., Toker, M., Gokce, E., Ustuner, B., Onder, N., Sagirkaya, H., et al., Successful ram semen cryopreservation with lyophilized egg yolk-based extender, *Cryobiology*, 2015, vol. 71, pp. 329–333. <https://doi.org/10.1016/j.cryobiol.2015.08.008>
  6. Pegg, D., The history and principles of cryopreservation, *Semin. Reprod. Med.*, 2002, vol. 20, pp. 5–13. <https://doi.org/10.1055/s-2002-23515>
  7. Alcay, S., Çakmak, S., Çakmak, I., Mulkpınar, E., Toker, M., Üstuner, B., Şen, H., and Nur, Z., Drone semen cryopreservation with protein supplemented TL-Hepes Based Extender, *Kafkas Univ. Vet. Fak. Derg.*, 2019a, vol. 25, no. 4, pp. 553–557. <https://doi.org/10.9775/kvfd.2018.21311>
  8. Bucak, M., Sariozkan, S., Tuncer, P., Sakin, F., Atesahin, A., Kulaksiz, R., et al., The effect of antioxidants on post-thawed Angora goat (*Capra hircus ancyrensis*) sperm parameters, lipid peroxidation and antioxidant activities, *Small Ruminant Res.*, 2010, vol. 8, no. 1, pp. 924–930. <https://doi.org/10.1016/j.smallrumres.2009.11.015>
  9. Nur, Z., Zik, B., Ustuner, B., Sagirkaya, H., and Ozguden, C., Effects of different cryoprotective agents on ram sperm morphology and DNA integrity, *Theriogenology*, 2010, vol. 73, pp. 1267–1275. <https://doi.org/10.1016/j.theriogenology.2009.12.007>
  10. Gravance, C., Vishwanath, R., Pitt, C., Garner, D., and Casey, P., Effects of cryopreservation on bull sperm head morphometry, *J. Androl.*, 1998, vol. 19, pp. 704–709. <https://onlinelibrary.wiley.com/doi/pdf/10.1002/j.1939-4640.1998.tb02079.x>
  11. Thompson, L., Brook, P., Warren, M., Barratt, C.L.R., and Cooke, I., A morphometric comparison of the nuclear morphology of fresh and frozen-thawed human zona-bound and unbound sperm, *J. Androl.*, 1994, vol. 15, pp. 337–342. <https://pubmed.ncbi.nlm.nih.gov/7982802/>
  12. Arruda, R., Ball, B., Gravance, C., Garcia, A., and Liu, I.K.M., Effects of extenders and cryoprotectants on stallion sperm head morphology, *Theriogenology*, 2002, vol. 58, pp. 253–256. <https://www.researchgate.net/publication/286954661>
  13. Rijsselaere, T., Van Soom, A., Hoflack, G., Maes, D., and de Kruif, A., Automated sperm morphometry and morphology analysis of canine semen by the Hamilton-Thorne analyzer, *Theriogenology*, 2004, vol. 62, pp. 1292–1306. <https://doi.org/10.1016/j.theriogenology.2004.01.005>
  14. Estes, M., Fernández-Santos, M., Soler, A., Montoro, V., Quintero-Moreno, A., and Garde, J., The effects of cryopreservation on the morphometric dimensions of Iberian Red Deer (*Cervus elaphus hispanicus*) epididymal sperm heads, *Reprod. Domest. Anim.*, 2006, vol. 41, pp. 241–246. <https://doi.org/10.1111/j.1439-0531.2006.00676.x>
  15. Gravance, C., White, C., Robertson, K., Champion, Z., and Casey, P., The effects of cryopreservation on the morphometric dimensions of caprine sperm heads, *Anim. Reprod. Sci.*, 1997, vol. 49, pp. 37–43. <https://kunderdoc.com/download/>
  16. Duncan, W., Glew, M., Wang, X., Flaherty, S., and Matthews, C., Prediction of fertilization rates from semen variables, *Fertil. Steril.*, 1993, vol. 59, pp. 1233–1238. [https://doi.org/10.1016/s0015-0282\(16\)55982-2](https://doi.org/10.1016/s0015-0282(16)55982-2)
  17. Hinting, A., Comhaire, F., Vermeulen, L., Dhort, M., Vermeulen, A., and Vanderbergh, D., Value of sperm characteristics and the result of *in vitro* fertilization for predicting the outcome of assisted reproduction, *Int. J. Androl.*, 1990, vol. 13, pp. 59–64. <https://doi.org/10.1111/j.1365-2605.1990.tb00960.x>
  18. Atroshchenko, M., Kalaschnikov, V., Bragina, E.E., and Zaitsev, A.M.A., Comparative study of the structural integrity of spermatozoa in epididymal, ejaculated and cryopreserved semen of stallions, *S-kh. Biol.*, 2017, vol. 52, no. 2, pp. 274–281. <https://doi.org/10.15389/agrobiol.2017.2.274rus>
  19. Kandiel, M.M.M., El-Khawagah, A.R.M., et al., Quantitative ultrastructure evaluation of Egyptian buffalo bull frozen-thawed spermatozoa under the effect of honey, *Scholars J. Agric. Vet. Sci.*, 2019, vol. 6, no. 3, pp. 92–98. <https://doi.org/10.21276/sjavs.2019.6.3.4>
  20. Silva, A., Fontenele-Neto, J., Cardoso, R., Silva, L., Chirinéa, V., and Lopes, M., Description of ultrastructural damages in frozen-thawed canine spermatozoa, *Ciência Animal Brasileira*, 2009, vol. 10, no. 2, pp. 595–601. [https://www.researchgate.net/publication/43530499\\_](https://www.researchgate.net/publication/43530499_)
  21. Laidlaw, H., *Instrumental insemination of honey bee queens: pictorial instruction manual*, Hamilton: Dadant & Son, 1997.
  22. Bagirov, V., Voyevodin, V., Klenovitskiy, P., Iolchiyev, B., Zhilinskiy, M., and Shaydullin, I., Increase in cryostability of goat buck semen as a result of removal of seminal plasma by filtration, *Altai State Agrar. Univ. Bull.*, 2017, vol. 9, no. 155, pp. 148–154.
  23. Tadzhiyeva, A., Iolchiyev, B., and Trebunskiy, A., Breed of boars and morphometric parameters of spermatozoa, in *Materials of the International Scientific Conference. VIJ Named after L.K. Ernst*, Moscow, 2019, pp. 216–252. <https://vitrina.vij.ru/sborniki/item/sovremennye-dostizheniya-i-problemy-genetiki-i-biotekhnologii-v-zhivotnovodstve>
  24. Zaghoul, A., Relevance of honey bee in semen extender on the quality of chilled-stored ram semen, *J. Anim. Poultry Prod.*, 2017, vol. 8, no. 1, pp. 1–5. <https://doi.org/10.21608/jappmu.2017.45740>
  25. Locke, S., Peng, Y., and Cross, N., A supravital staining technique for honey bee spermatozoa, *Physiol. Entomol.*, 1990, vol. 15, pp. 187–192. <https://doi.org/10.1111/j.1365-3032.1990.tb00506.x>
  26. Rhodes, J., Semen production in drone honeybees, in *Rural Industries Research and Development Corporation*, Australia, 2008, vol. 08. <https://rirdc.infoservices.com.au/downloads/08-130>. Cited January 8, 2013.



27. Lensky, Y., Ben-David, E., and Schindler, H., Ultrastructure of the spermatozoon of the mature drone honeybee, *J. Apic. Res.*, 1979, vol. 18, no. 4, pp. 264–271.
28. Lino-Neto, J., Bão, S., and Dolder, H., Sperm ultrastructure of the honey bee (*Apis mellifera*) (L) (Hymenoptera, Apidae) with emphasis on the nucleus flagellum transition region, *Tissue Cell*, 2000, vol. 32, no. 4, pp. 322–327. <http://www.idealibrary.com>. <https://doi.org/10.1054/tice.2000.0119>
29. Woyke, J., Ultrastructure of single and multiple diploid honeybee spermatozoa, *J. Apic. Res.*, 1984, vol. 23, no. 3, pp. 123–135.
30. Peng, C., Yin, C.M., and Yin, L.R.S., Ultrastructure of honey bee, *Apis mellifera*, sperm with special emphasis on the acrosomal complex following high-pressure freezing fixation, *Physiol. Entomol.*, 1993, vol. 18, pp. 93–101. <https://doi.org/10.1111/j.1365-3032.1993.tb00454.x>
31. Gontarz, A., Banaszewska, D., Gryzinska, M., and Andraszek, K., Differences in drone sperm morphometry and activity at the beginning and end of the season, *Turk. J. Vet. Anim. Sci.*, 2016, vol. 40, pp. 598–602. <https://doi.org/10.3906/vet-1511-6>
32. Power, K., D'Anza, E., Martano, M., Albarella, S., Ciotola, F., Peretti, F., and Maiolino, P., Morphological and morphometric analysis of the Italian honeybee (*Apis mellifera ligustica*) spermatozoa: a preliminary study in Campania region, *Vet. Med. Anim. Sci.*, 2019, vol. 6, pp. 1–4. <https://doi.org/10.7243/2054-3425-6-2>
33. Gil, M., Garcia-Herreros, M., Baron, F., Aparicio, I., Santos, A., and Garcia-Marin, L., Morphometry of porcine spermatozoa and its functional significance in relation with the motility parameters in fresh semen, *Theriogenology*, 2009, vol. 71, pp. 254–263. <https://doi.org/10.1016/j.theriogenology.2008.07.007>
34. Hopkins, B. and Herr, C., Factors affecting the successful cryopreservation of honey bee (*Apis mellifera*) spermatozoa, *Apidologie*, 2010, vol. 41, pp. 548–556. <https://doi.org/10.1051/apido/20010006>
35. Alçay, S., Çakmak, S., Çakmak, I., Mulkpınar, E., Gökçe, E., Üstüner, B., Şen, H., and Nur, Z., Successful cryopreservation of honey bee drone spermatozoa with royal jelly supplemented extenders, *Cryobiology*, 2019b., vol. 87, pp. 28–31. <https://doi.org/10.1016/j.cryobiol.2019.03.005>
36. Wegener, J., May, T., Kamp, G., and Bienefeld, K., A successful new approach to honeybee semen cryopreservation, *Cryobiology*, 2014, vol. 69, pp. 236–242. <https://doi.org/10.1016/j.cryobiol.2014.07.011>
37. Royere, D., Hamamah, S., Nicolle, J., Barthelemy, C., and Lansac, I., Freezing and thawing alter chromatin stability of ejaculated human spermatozoa: fluorescence acridine orange staining and Fielgen-DNA cytophotometric studies, *Gamete Res.*, 1988, vol. 21, pp. 51–57. <https://doi.org/10.1002/mrd.1120210107>
38. England, G., Cryopreservation of dog semen: a review, *J. Reprod. Fertil. Suppl.*, 1993, vol. 47, pp. 243–255. <https://pubmed.ncbi.nlm.nih.gov/8229932/>. Cited April 27, 2021.
39. Zampini, R., Castro-González, X., Sari, L., Martin, A., Diaz, A., Argañaraz, M., and Apichela, S., Effect of cooling and freezing on Llama (*Lama glama*) sperm ultrastructure, *Front. Vet. Sci.*, 2020, vol. 7, pp. 1–14. <https://doi.org/10.3389/fvets.2020.587596>
40. Balamurugan, R., Prapaporn, W., and Munuswamy, N., Sperm activation and effects of cryopreservation on motility, ultrastructure and DNA integrity in Grey mullet *Mugil cephalus*, *Aquacult. Rep.*, 2019, vol. 14, pp. 1–9. <https://doi.org/10.1016/j.aqrep.2019.100204>
41. Keskin, N., Erdogan, C., Numan Bucak, M., Erdem Ozturk, A., Bodu, M., Ili, P., Baspınar, N., and Dursun, S., Cryopreservation effects on ram sperm ultrastructure, *Biopreserv. Biobanking*, 2020, vol. 18, no. 5, pp. 441–448. <https://doi.org/10.1089/bio.2020.0056>